

# The direct synthesis of dimethyl ether from syngas over hybrid catalysts with sulfate-modified $\gamma$ -alumina as methanol dehydration components

Dongsen Mao<sup>a,b,\*</sup>, Weimin Yang<sup>b</sup>, Jianchao Xia<sup>b</sup>, Bin Zhang<sup>b</sup>, Guanzhong Lu<sup>a</sup>

<sup>a</sup> Department of Chemical Engineering, Shanghai Institute of Technology, Shanghai 200235, PR China

<sup>b</sup> Shanghai Research Institute of Petrochemical Technology, SINOPEC, Shanghai 201208, PR China

Received 20 May 2005; received in revised form 24 January 2006; accepted 24 January 2006

Available online 28 February 2006

## Abstract

A series of  $\gamma$ -Al<sub>2</sub>O<sub>3</sub> samples modified with various contents of sulfate (0–15 wt.%) and calcined at different temperatures (350–750 °C) were prepared by an impregnation method and physically admixed with CuO–ZnO–Al<sub>2</sub>O<sub>3</sub> methanol synthesis catalyst to form hybrid catalysts. The direct synthesis of dimethyl ether (DME) from syngas was carried out over the prepared hybrid catalysts under pressurized fixed-bed continuous flow conditions. The results revealed that the catalytic activity of SO<sub>4</sub><sup>2-</sup>/ $\gamma$ -Al<sub>2</sub>O<sub>3</sub> for methanol dehydration increased significantly when the content of sulfate increased to 10 wt.%, resulting in the increase in both DME selectivity and CO conversion. However, when the content of sulfate of SO<sub>4</sub><sup>2-</sup>/ $\gamma$ -Al<sub>2</sub>O<sub>3</sub> was further increased to 15 wt.%, the activity for methanol dehydration was increased, and the selectivity for DME decreased slightly as reflected in the increased formation of byproducts like hydrocarbons and CO<sub>2</sub>. On the other hand, when the calcination temperature of SO<sub>4</sub><sup>2-</sup>/ $\gamma$ -Al<sub>2</sub>O<sub>3</sub> increased from 350 °C to 550 °C, both the CO conversion and the DME selectivity increased gradually, accompanied with the decreased formation of CO<sub>2</sub>. Nevertheless, a further increase in calcination temperature to 750 °C remarkably decreased the catalytic activity of SO<sub>4</sub><sup>2-</sup>/ $\gamma$ -Al<sub>2</sub>O<sub>3</sub> for methanol dehydration, resulting in the significant decline in both DME selectivity and CO conversion. The hybrid catalyst containing the SO<sub>4</sub><sup>2-</sup>/ $\gamma$ -Al<sub>2</sub>O<sub>3</sub> with 10 wt.% sulfate and calcined at 550 °C exhibited the highest selectivity and yield for the synthesis of DME.

© 2006 Published by Elsevier B.V.

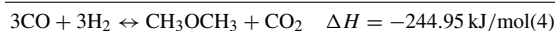
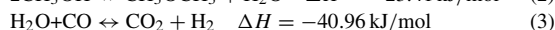
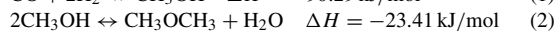
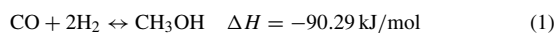
**Keywords:** Syngas; Dimethyl ether; Hybrid catalyst; Dehydration of methanol; Sulfate-modified  $\gamma$ -Al<sub>2</sub>O<sub>3</sub>

## 1. Introduction

Dimethyl ether (DME) is a key intermediate for the production of many important chemicals such as dimethyl sulfate, methyl acetate and light olefins [1,2]. In addition, DME has been increasingly used as an aerosol propellant to replace chlorofluorocarbons, which were found to destroy the ozone layer of the atmosphere [3]. Most importantly, DME has recently received a world-wide attention since it has a great potential as a clean alternative fuel for diesel engines because of its thermal efficiencies equivalent to traditional diesel fuel, much lower NO<sub>x</sub> emission, less carbon particulates, near-zero smoke production and less engine noise [4].

In view of the potential of DME as a clean alternative diesel fuel, much consideration should be paid to the production of DME in large quantities. Presently, DME is produced in small

quantities by methanol dehydration over solid acid catalysts such as  $\gamma$ -alumina and zeolite HZSM-5, while methanol is synthesized from syngas over Cu-based oxide catalysts (e.g., CuO/ZnO/Al<sub>2</sub>O<sub>3</sub>). In methanol synthesis, conversion of syngas to methanol is determined by the thermodynamic equilibrium; therefore, high pressure and low temperature are highly desired for the reaction. In the 1980s, a method called syngas to DME (STD) process was developed for the direct production of DME from syngas over a hybrid catalyst, which is composed of a methanol synthesis catalyst and a solid acid catalyst [5]. Compared to the conventional method, the STD process is attracting more and more industrial and academic attention for its dramatically economic values and theoretical significance. The principal reactions involved in the STD process are methanol synthesis, methanol dehydration and WGS (water gas shift) [6]:



\* Corresponding author. Tel.: +86 21 64945006; fax: +86 21 64945006.

E-mail address: [dsmao@sit.edu.cn](mailto:dsmao@sit.edu.cn) (D. Mao).

The combination of these reactions results in a synergistic effect of relieving the unfavorable thermodynamics for methanol synthesis: methanol, product in reaction (1), is consumed for reaction (2) to DME and water. The water is shifted by the WGS reaction (3) to form carbon dioxide and hydrogen, the latter being a reactant for reaction (1). Therefore, one of the products of each step is a reactant for another. This creates a strong driving force for the overall reaction which allows a very high syngas conversion in one single pass.

Up to now, the most common hybrid catalysts reported in the literature for the STD process are the physical mixture of the methanol synthesis catalyst and the solid acid catalyst [2,5,7–11]. The Cu/ZnO-based catalyst has been used successfully for several decades for the production of methanol from syngas, and the reaction mechanism and the role of each active ingredient of the catalyst have been well studied [12–14]. Compared with that for methanol synthesis, the study on the catalyst for methanol dehydration has received less attention. To date, only a few solid acids such as  $\gamma$ -Al<sub>2</sub>O<sub>3</sub> [5,8–10,15–20], silica-alumina [7] and zeolites like HZSM-5 [10,11,21–23], HY [2,21,24] and HMCM-49 [25] have been used as methanol dehydration catalysts for the STD process. Among them,  $\gamma$ -Al<sub>2</sub>O<sub>3</sub> has been mostly employed due to its low price, easy availability and high stability. However, it is well established in the literature that at the optimum reaction temperature (ca. 260 °C) for the methanol synthesis process the activity of  $\gamma$ -Al<sub>2</sub>O<sub>3</sub> for methanol dehydration was rather poor [7,26]. On the other hand, the reactions involved in the STD process are made all thermodynamically unfavorable by the increase in reaction temperature. Furthermore, the sintering of copper of the Cu-based methanol synthesis component at high temperatures would lead to deactivation of the hybrid catalyst. Hence, the modification of  $\gamma$ -Al<sub>2</sub>O<sub>3</sub> to increase its catalytic activity for methanol dehydration reaction at the optimum reaction temperature for the methanol synthesis process has become a very important step to improve the selectivity to DME and the conversion of syngas [10].

It has been reported that a 1 wt.% titania-modified  $\gamma$ -Al<sub>2</sub>O<sub>3</sub> catalyst exhibits a higher activity for methanol dehydration than the commonly used phosphoric acid modified  $\gamma$ -Al<sub>2</sub>O<sub>3</sub> [27]. However, the optimum operating temperature (ca. 400 °C) over TiO<sub>2</sub>-modified  $\gamma$ -Al<sub>2</sub>O<sub>3</sub> is still significantly higher than that employed in the STD process [26]. On the other hand, Xu et al. [26] found that TiO<sub>2</sub> modified  $\gamma$ -Al<sub>2</sub>O<sub>3</sub> exhibited comparable activity to  $\gamma$ -Al<sub>2</sub>O<sub>3</sub>. Recently, Jun et al. [28] found that  $\gamma$ -Al<sub>2</sub>O<sub>3</sub> modified with 1 wt.% SiO<sub>2</sub> is more active than the unmodified one; the increase in the conversion of methanol at 250 °C reaches as high as 10%. Very recently, Baghaei and co-workers [29] also reported that the silica modified  $\gamma$ -Al<sub>2</sub>O<sub>3</sub> catalysts showed better performance for the methanol dehydration reaction than the untreated  $\gamma$ -Al<sub>2</sub>O<sub>3</sub>, in which the sample with 6 wt.% silica loading exhibited the best methanol conversion.

It has also been well demonstrated in the literature that sulfate treatment can increase the acidity of  $\gamma$ -Al<sub>2</sub>O<sub>3</sub>. For example, Berteau and Delmon [30] reported that the sulfate ions incorporated into alumina increased the amount of acid sites from 0.73 mmol g<sup>-1</sup> to 1.23 mmol g<sup>-1</sup>. Curtin et al. [31]

also found that sulfate modification considerably increased the acid sites concentration of  $\gamma$ -Al<sub>2</sub>O<sub>3</sub> from 4.0 mmol m<sup>-2</sup> to 18.3 mmol m<sup>-2</sup>. Furthermore, sulfated  $\gamma$ -Al<sub>2</sub>O<sub>3</sub> has even been considered to possess superacidic sites and used as catalysts for the benzylation of toluene with benzoyl chloride or benzoic anhydride [32], the isomerization of alkane such as *n*-butane [33] and pentane [34,35]. Very recently, however, Gawthrop and Lee [36] found that sulfation did increase the surface acidity of  $\gamma$ -Al<sub>2</sub>O<sub>3</sub>, but sulfated aluminas did not show superacidity in contrast to their sulfated zirconia counterparts. Surprisingly, despite its wide use for catalytic reactions, to the best of our knowledge, sulfate-promoted alumina has not been exploited to catalyze the dehydration of methanol in the STD process up to now [37,38].

In the present paper, we report results for the direct synthesis of DME from syngas over the hybrid catalysts with sulfate-modified  $\gamma$ -Al<sub>2</sub>O<sub>3</sub> as methanol dehydration components for the first time. The acidic properties of the SO<sub>4</sub><sup>2-</sup>/ $\gamma$ -Al<sub>2</sub>O<sub>3</sub> samples with various sulfate contents and calcined at different temperatures were measured and correlated with their catalytic performance; and the lifetime of the most active and selective catalyst was also examined.

## 2. Experimental

### 2.1. Catalyst preparation

A commercial  $\gamma$ -Al<sub>2</sub>O<sub>3</sub> was used as starting material. Sulfate-modified  $\gamma$ -Al<sub>2</sub>O<sub>3</sub> samples with various sulfate contents were prepared by wet impregnation of  $\gamma$ -Al<sub>2</sub>O<sub>3</sub> with an aqueous solution containing a suitable amount of (NH<sub>4</sub>)<sub>2</sub>SO<sub>4</sub> (Analytical Grade, Shanghai Chemical Reagent Corporation, China), followed by drying at 110 °C overnight and then calcined at different temperatures (350–750 °C) for 3 h in an air stream. This series of samples is designated as *x*-SA-*T*, where *x* and *T* stands for the weight percentage of sulfate ion and calcination temperature in °C, respectively. The reference sample was prepared following the same procedure, but without (NH<sub>4</sub>)<sub>2</sub>SO<sub>4</sub> added. The reference alumina was designated as A.

The CuO–ZnO–Al<sub>2</sub>O<sub>3</sub> (Cu:Zn:Al = 6:3:1 atomic ratio) methanol synthesis catalysts were prepared by the conventional coprecipitation method, wherein a mixed aqueous solution of Cu(NO<sub>3</sub>)<sub>2</sub>·3H<sub>2</sub>O, Zn(NO<sub>3</sub>)<sub>2</sub>·6H<sub>2</sub>O, and Al(NO<sub>3</sub>)<sub>3</sub>·9H<sub>2</sub>O and an aqueous solution of Na<sub>2</sub>CO<sub>3</sub> were added simultaneously. Good reproducibility and comparability of the catalysts was achieved by controlling the preparation conditions (i.e. the pH value, stirring velocity, duration of precipitation, aging, etc.) carefully. The resultant precipitate was filtered off and washed with a hot NH<sub>4</sub>NO<sub>3</sub> solution followed by washing with sufficient deionized water to remove residual sodium ions. The solid obtained was dried at 110 °C overnight and then calcined at 350 °C in flowing air for 6 h.

The hybrid catalysts used for the STD reaction were prepared by physically mixing the methanol synthesis catalysts CuO–ZnO–Al<sub>2</sub>O<sub>3</sub> and the parent and sulfate-modified  $\gamma$ -Al<sub>2</sub>O<sub>3</sub> catalysts (2:1 by weight). Before mixing they were separately tableted and pulverized into granules (20–40 mesh).

## 2.2. Catalyst characterization

The surface areas of the samples were analyzed by the  $N_2$  adsorption method at  $-196^\circ\text{C}$  with a Micromeritics TriStar 3000 surface area analyzer. Samples were outgassed under vacuum to remove the physisorbed moisture prior to analysis.

The sulfate content in each sample was determined gravimetrically on a thermal analysis system (Perkin Elmer, TGA-7). After 30 min of dehydration at  $400^\circ\text{C}$ , the sample temperature was linearly raised to  $1200^\circ\text{C}$  at a rate of  $10^\circ\text{C min}^{-1}$  in a  $N_2$  flow ( $100\text{ ml min}^{-1}$ ). Pure  $\gamma\text{-Al}_2\text{O}_3$  was used as a blank in the reference port to compensate the possible interference from the dehydration on the surface of  $\gamma\text{-Al}_2\text{O}_3$ . The sulfate content of the testing sample was estimated from the weight loss ( $\Delta m$ ) between  $400^\circ\text{C}$  and  $1200^\circ\text{C}$  in the TGA profiles. The DTG profiles were obtained by differentiating the TGA profiles.

Acidity measurements were performed by temperature-programmed desorption of ammonia ( $\text{NH}_3$ -TPD) using a conventional flow apparatus equipped with a thermal conductivity detector (TCD). A given amount of the sample (0.1 g) was pre-treated in flowing helium (He) at  $550^\circ\text{C}$  for 1 h, cooled to  $150^\circ\text{C}$  and then exposed to  $\text{NH}_3$  ( $20\text{ ml min}^{-1}$ ) for 30 min. The sample adsorbed by  $\text{NH}_3$  was subsequently purged with He gas at the same temperature for 1 h to remove the physisorbed  $\text{NH}_3$ . The TPD measurement was conducted in flowing He gas ( $30\text{ ml min}^{-1}$ ) from  $150^\circ\text{C}$ , at a heating rate of  $10^\circ\text{C min}^{-1}$ , to  $550^\circ\text{C}$  and hold it at this temperature for 30 min. The evolved ammonia was trapped in a dilute  $\text{H}_2\text{SO}_4$  solution ( $0.005\text{ mol L}^{-1}$ ) located at the down-stream of the flow. Its total amount was determined by back-titration of excess sulfuric acid with a dilute NaOH solution ( $0.01\text{ mol L}^{-1}$ ).

## 2.3. Reaction studies

The catalytic activity test was carried out in a fixed-bed flow reactor constructed of a 6 mm i.d. stainless steel tube and equipped with a thermocouple in the catalyst bed. The pressure in the reactor was maintained by means of a back pressure regulator (GO Inc., USA) and the flow rate of syngas was controlled by a mass flow controller (Brooks 5850E, Japan). Prior to reaction, the hybrid catalysts (1 g) were reduced by hydrogen (5 vol.% in nitrogen) in situ at  $240^\circ\text{C}$  for 6 h. The syngas (pre-mixed) contained 66%  $\text{H}_2$ , 30%  $\text{CO}$  and 4%  $\text{CO}_2$ . The reaction was performed under the reaction conditions of 4 MPa, the feed rate of  $1500\text{ mL h}^{-1}\text{g}_{\text{cat}}^{-1}$ , and the temperature of  $260^\circ\text{C}$ . Effluent gas from the reactor was heated electrically on-line to avoid the condensation of the products, and analyzed by an on-line gas chromatograph (HP 4890D) equipped with a Carbosphere column connected to a thermal conductivity detector (TCD) for  $\text{CO}_2$  and  $\text{CO}$ , and with a Porapark N column connected to a flame ionization detector (FID) for methanol, DME and light hydrocarbons. All data were obtained under steady-state conditions that were usually maintained for 4 h. As measures of the catalytic activity, the conversion of  $\text{CO}$  and the selectivity of the products were used and calculated according to literature [39].

Table 1

Sulfate contents, surface areas and acid amounts of the  $\text{SO}_4^{2-}/\gamma\text{-Al}_2\text{O}_3$  samples

Sample	Surface area	Sulfate content <sup>a</sup> (wt.%)	Acidity <sup>b</sup>	
			$\mu\text{mol m}^{-2}$	$\text{mmol g}^{-1}$
A	297.7	–	0.98	0.29
5-SA-550	281.5	6.48	1.80	0.51
10-SA-550	316.6	9.28	2.38	0.76
15-SA-550	304.5	11.12	2.69	0.82
10-SA-350	294.7	–	2.87	0.85
10-SA-450	297.7	–	2.44	0.73
10-SA-650	277.4	7.64	2.55	0.71
10-SA-750	173.8	4.04	2.54	0.44

<sup>a</sup> Determined by TGA.<sup>b</sup> Determined by  $\text{NH}_3$ -TPD.

## 3. Results and discussion

### 3.1. Characterization of $\text{SO}_4^{2-}/\gamma\text{-Al}_2\text{O}_3$

Table 1 shows the BET surface areas of the different  $\text{SO}_4^{2-}/\gamma\text{-Al}_2\text{O}_3$  samples. It can be seen that the 10-SA-550 sample exhibits the highest value. The remarkable decrease in surface area observed over the samples calcined at higher temperatures (particularly at  $750^\circ\text{C}$ ) may be caused by the collapse of pores.

Fig. 1 presents the DTG profiles of the different  $\text{SO}_4^{2-}/\gamma\text{-Al}_2\text{O}_3$  samples. For the 5-SA-550 sample, a peak at around  $900^\circ\text{C}$  appeared, which is due to the evolution of  $\text{SO}_3$  decomposed from the sulfate ion bonded to the surface of  $\gamma\text{-Al}_2\text{O}_3$  [33,34]. As the sulfate content increased, the peak width progressively became broadened toward lower temperatures, indicating that different sulfate species was formed in the samples. When the sulfate content increased to 15 wt.%, the peak maximum appeared at  $730^\circ\text{C}$ . The peak at the lower temperature can be assigned to the decomposition of sulfate exceeding a monolayer

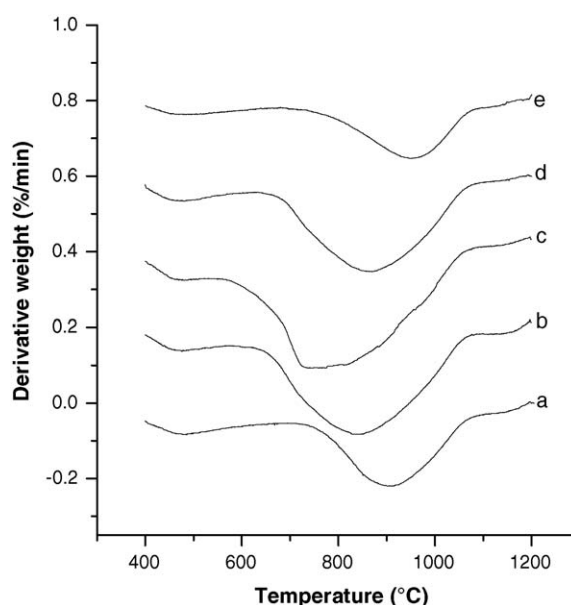


Fig. 1. DTG patterns of the various  $\text{SO}_4^{2-}/\gamma\text{-Al}_2\text{O}_3$  samples: (a) 5-SA-550, (b) 10-SA-550, (c) 15-SA-550, (d) 10-SA-650 and (e) 10-SA-750.

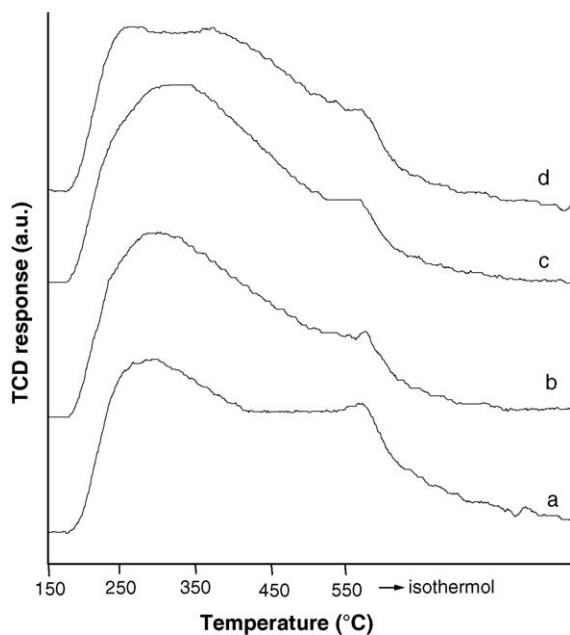


Fig. 2.  $\text{NH}_3$ -TPD profiles of the  $\text{SO}_4^{2-}/\gamma\text{-Al}_2\text{O}_3$  samples calcined at  $550^\circ\text{C}$  with various  $\text{SO}_4^{2-}$  contents: (a) 0, (b) 5 wt.%, (c) 10 wt.% and (d) 15 wt.%.

on the surface of  $\gamma\text{-Al}_2\text{O}_3$ . The result obtained here and those in the literature [33,34] are in contradiction with that on  $\text{NiSO}_4/\gamma\text{-Al}_2\text{O}_3$  reported by Sohn and Park [40], who assigned the lower temperature peak to the decomposition of surface sulfate while the higher temperature peak to multilayer sulfate. On the other hand, the peak position of the decomposition shifted to higher temperatures with an increase in calcination temperature for the preparation of  $\text{SO}_4^{2-}/\gamma\text{-Al}_2\text{O}_3$ . Especially, when the calcination temperature was raised to  $750^\circ\text{C}$ , the peak width substantially sharpened toward a higher temperature; the peak was located at  $950^\circ\text{C}$ . These results suggest that the interaction strengths of the different sulfate species with  $\gamma\text{-Al}_2\text{O}_3$  are different: the surface sulfates have a stronger interaction than the multilayer ones.

The surface acidic properties of the  $\gamma\text{-Al}_2\text{O}_3$  and  $\text{SO}_4^{2-}/\gamma\text{-Al}_2\text{O}_3$  samples with various sulfate contents calcined at  $550^\circ\text{C}$  were determined by  $\text{NH}_3$ -TPD; the results are depicted in Fig. 2. It can be seen that a peak maximum appeared in every TPD profile slightly beyond  $550^\circ\text{C}$ , at which the heating program was switched off. This phenomenon was also observed by other researchers [41,42]. As Chang and Ko [42] suggested, this is probably due to the effect of increasing and then decreasing temperature since a TCD detector was used in monitoring desorbed ammonia. Apart from the peak at  $550^\circ\text{C}$ , the  $\text{NH}_3$ -TPD profile of  $\gamma\text{-Al}_2\text{O}_3$  (Fig. 2a) exhibited a broad peak with maximum at about  $290^\circ\text{C}$ . After sulfate modification, the peak maximum was shifted to higher temperatures, indicating that the acid strength of the  $\gamma\text{-Al}_2\text{O}_3$  was increased by sulfate addition. This result was consistent with those of previous reports [33–36,43]. Specifically, when the sulfate content was 5 wt.% and 10 wt.%, the peak maximum appeared at about  $300^\circ\text{C}$  and  $320^\circ\text{C}$ , respectively. At the highest content of 15 wt.% examined here, two  $\text{NH}_3$ -desorption peaks were observed: one appeared around  $260^\circ\text{C}$  and the other was located at about  $370^\circ\text{C}$ . The total amount

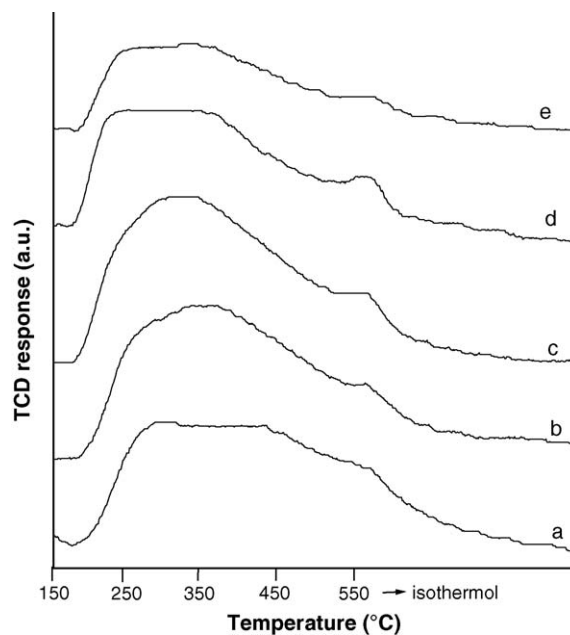


Fig. 3.  $\text{NH}_3$ -TPD profiles of the  $\text{SO}_4^{2-}/\gamma\text{-Al}_2\text{O}_3$  samples with 10 wt.% sulfate calcined at various temperatures: (a)  $350^\circ\text{C}$ , (b)  $450^\circ\text{C}$ , (c)  $550^\circ\text{C}$ , (d)  $650^\circ\text{C}$  and (e)  $750^\circ\text{C}$ .

of acid sites of every sample is shown in Table 1. The results of  $\text{NH}_3$ -TPD measurement suggest that both the number and strength of the acid sites of  $\gamma\text{-Al}_2\text{O}_3$  were increased by sulfate modification and increased gradually with sulfate content.

Fig. 3 displays the TPD profiles of ammonia desorbed from the  $\text{SO}_4^{2-}/\gamma\text{-Al}_2\text{O}_3$  samples with the same sulfate content (10 wt.%) but calcined at different temperatures. It is evident that the acid strength of the samples decreased with the increase in calcination temperature, which was indicated by a shift of the desorption peak of maximum height to lower desorption temperatures. As shown in Fig. 3, when the calcination temperature was not higher than  $450^\circ\text{C}$ , the peak maximum occurred at about  $350^\circ\text{C}$ . At a higher calcination temperature of  $550^\circ\text{C}$ , the desorption maximum decreased to  $320^\circ\text{C}$ . Particularly, when the calcination temperature was further increased to  $\geq 650^\circ\text{C}$ , the peak maximum decreased to  $300^\circ\text{C}$ . This result can be attributed to the loss of  $\text{SO}_4^{2-}$  existing in the samples calcined at higher temperatures, as shown in Table 1. On the other hand, the total area of the TPD peak decreased monotonously with an increase in the calcination temperature, indicating a decrease in the total number of acid sites. However, since the increase in calcination temperature from  $550^\circ\text{C}$  to  $750^\circ\text{C}$  also resulted in the decrease in the surface areas of the  $\text{SO}_4^{2-}/\gamma\text{-Al}_2\text{O}_3$  samples, the concentration of acid sites (per  $\text{m}^2$  sample), which was calculated by dividing the total number of  $\text{NH}_3$  by the BET surface area of the sample and also summarized in Table 1, was almost the same. Hence, the decrease in the numbers of acid sites over the  $\text{SO}_4^{2-}/\gamma\text{-Al}_2\text{O}_3$  samples calcined at higher temperatures ( $\geq 550^\circ\text{C}$ ) was caused by the decline of surface area. In summary, as shown in Fig. 3 and Table 1, it is clear that both the number and strength of the acid sites of the  $\text{SO}_4^{2-}/\gamma\text{-Al}_2\text{O}_3$  samples decreased with increasing calcination temperature.



Table 2  
DME synthesis directly from syngas on the hybrid catalysts containing sulfate-modified aluminas with various sulfate contents<sup>a</sup>

Sulfate content (wt.%)	CO conversion (C-mol%)	Selectivity (C-mol%)				DME yield (C-mol%)
		DME	Methanol	Hydrocarbons	CO <sub>2</sub>	
–	85.1	49.9	17.8	0.04	32.3	42.5
5	90.4	52.3	15.4	0.06	32.2	47.3
10	94.7	61.6	6.0	0.09	32.3	58.3
15	94.9	60.3	5.5	0.14	34.1	57.2

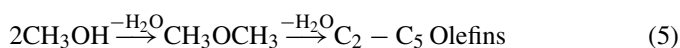
<sup>a</sup> Reaction conditions:  $T = 260\text{ }^{\circ}\text{C}$ ,  $P = 4\text{ MPa}$ ,  $\text{H}_2/\text{CO} = 2.2$ ,  $\text{CO}_2 = 4\%$ ,  $\text{GHSV} = 1500\text{ ml h}^{-1}\text{ g}^{-1}$ .

### 3.2. Catalytic activity

#### 3.2.1. Effect of sulfate content of $\text{SO}_4^{2-}/\gamma\text{-Al}_2\text{O}_3$

The hybrid catalysts containing the parent and sulfate-modified aluminas with various sulfate contents as methanol dehydration components were evaluated under the same reaction conditions; the results are summarized in Table 2. It can be noted that a high selectivity to methanol was found on the hybrid catalyst with the parent  $\gamma\text{-Al}_2\text{O}_3$ , indicating its low catalytic activity for methanol dehydration reaction, which resulted in a low DME selectivity. At the same time, since the methanol produced was not efficiently converted to DME, the merit of the direct synthesis of DME from syngas cannot be fulfilled effectively, resulting in a low CO conversion. However, after sulfate modification of  $\gamma\text{-Al}_2\text{O}_3$ , the methanol selectivity decreased progressively with increasing sulfate content, implying that the catalytic activity of  $\gamma\text{-Al}_2\text{O}_3$  for methanol dehydration was remarkably increased by the sulfate modification. On the other hand, the DME selectivity increased with the sulfate content up to 10 wt.% and then decreased slightly as the content of sulfate was further increased accompanied with the increased selectivity to by-products like hydrocarbons and  $\text{CO}_2$ , although the selectivity to methanol was further decreased. Furthermore, the CO conversion increased with increasing sulfate content to 10 wt.% and remained practically constant above this content. Hence, a maximum of DME yield (58.3%) was obtained at the sulfate content of 10 wt.%. This value was close to the equilibrium yield of DME in our experimental conditions (ca. 65%) [25].

As the dehydration of methanol to form DME is a typical acidity dependent reaction [44], a higher acidity hints a higher catalytic activity [45]. However, it has been well demonstrated in the literature that the strong acid sites on catalyst surface can catalyze the further dehydration of the originally formed DME to low molecular weight olefins [46]. The general reaction scheme, which shows a consecutive reaction, can be outlined as follows [47]:



Moreover, Joo et al. [10] recently proposed that the strong acid sites may promote the water reforming reactions of methanol and dimethyl ether to produce carbon dioxide. Evidently, these side reactions caused by the strong acid sites will deteriorate the DME selectivity. Accordingly, the enhanced catalytic activity of  $\gamma\text{-Al}_2\text{O}_3$  for methanol dehydration after sulfate modification presented in this work can be attributed to the increase in both the

number and strength of acid sites, as shown in Fig. 2 and Table 1. On the other hand, because the acidity of  $\gamma\text{-Al}_2\text{O}_3$  was not strong enough to convert effectively the produced methanol to DME, the dehydration reaction became a rate-determining step. Therefore, the increment of acidity increased concurrently the DME selectivity and the CO conversion. This result is in line with the previous observation by Joo et al. [10], who reported that the increase in acidity on  $\gamma\text{-Al}_2\text{O}_3$  resulted in simultaneous increase of DME selectivity (from 64.1% to 79.5%) and CO conversion (from 52.8% to 67.0%). However, when the content of sulfate was increased to 15 wt.%, stronger acid sites appeared in the modified  $\gamma\text{-Al}_2\text{O}_3$  (see Fig. 2), which resulted in the increased formation of  $\text{CO}_2$  [10] and light olefins [46], the latter subsequently being hydrogenized to form the corresponding paraffins [8]. On one hand, these side reactions decreased the selectivity to DME. On the other hand, the increased formation of light hydrocarbons would induce quicker deactivation of the catalyst due to coking [26]. Consequently, the 10 wt.%  $\text{SO}_4^{2-}/\gamma\text{-Al}_2\text{O}_3$  catalyst with a larger number of acid sites of intermediate strength was the most favorable methanol dehydration component of the hybrid catalyst for the STD process. This result is in contradiction with the conclusion reached by Kim et al. [11] that the strong acid sites are responsible for the formation of DME while the relatively weak acid sites appearing below  $450\text{ }^{\circ}\text{C}$  in the  $\text{NH}_3\text{-TPD}$  spectra are not important for the dehydration of methanol to DME.

From the above results, it can be concluded that, in the STD process, when the acidity of the acidic component is not strong enough to convert effectively the originally produced methanol to DME, the dehydration reaction is the rate-determining step. In this case, the acidity of acid catalyst greatly affects both the CO conversion and the DME selectivity: the increase in the acidity of the acidic component will result in the improvement of both the DME selectivity and the CO conversion on the hybrid catalyst. On the other hand, if the acid catalysts are so active for methanol dehydration that the intrinsic methanol synthesis rate is much lower than the methanol dehydration rate, the overall reaction is determined by the methanol synthesis step (reaction (1)) rather than the DME formation itself (reaction (2)). In this case, the acidity of acid catalyst mainly affects the DME selectivity: the too strong acid sites promote the formation of larger amounts of by-products like hydrocarbons and  $\text{CO}_2$ , resulting in lower selectivity to the desired DME. This conclusion is similar to those obtained recently by Kim et al. [11] and Ramos et al. [48].

Table 3

DME synthesis directly from syngas on the hybrid catalysts containing sulfate-modified aluminas calcined at different temperatures<sup>a</sup>

Calcination temperature (°C)	CO conversion (C-mol%)	Selectivity (C-mol%)				DME yield (C-mol%)
		DME	Methanol	Hydrocarbons	CO <sub>2</sub>	
350	92.7	51.6	5.9	0.08	42.4	47.8
450	93.7	55.4	5.8	0.06	38.8	51.9
550	94.7	61.6	6.0	0.09	32.3	58.3
650	93.4	58.3	8.8	0.07	32.8	54.4
750	84.6	43.7	24.1	0.09	32.1	37.0

<sup>a</sup> Reaction conditions:  $T = 260\text{ }^{\circ}\text{C}$ ,  $P = 4\text{ MPa}$ ,  $\text{H}_2/\text{CO} = 2.2$ ,  $\text{CO}_2 = 4\%$ ,  $\text{GHSV} = 1500\text{ ml h}^{-1}\text{ g}^{-1}$ .

### 3.2.2. Effect of calcination temperature of $\text{SO}_4^{2-}/\gamma\text{-Al}_2\text{O}_3$

The performance of the hybrid catalysts using sulfate (10 wt.%) modified aluminas calcined at different temperatures as methanol dehydration components are compared in Table 3. It can be seen that, when the calcination temperature was  $\leq 550\text{ }^{\circ}\text{C}$ , the selectivity to  $\text{CO}_2$  decreased gradually with the increase in calcination temperature, accompanied with the enhancement of DME selectivity. Meanwhile, the equilibrium conversion of reaction (4) would shift toward the right-hand side because of the decrease in the formation of  $\text{CO}_2$ . Therefore, the CO conversion also increased distinctly with increasing the calcination temperature, even though the increase was small. As a result, the yield of DME increased significantly from ca. 48% for the  $\text{SO}_4^{2-}/\gamma\text{-Al}_2\text{O}_3$  calcined at  $350\text{ }^{\circ}\text{C}$  to ca. 58% for the  $\text{SO}_4^{2-}/\gamma\text{-Al}_2\text{O}_3$  calcined at  $550\text{ }^{\circ}\text{C}$ . On the other hand, when the calcination temperature was  $\geq 550\text{ }^{\circ}\text{C}$ , the selectivity to methanol increased gradually with the calcination temperature, indicating that the catalytic activity of  $\text{SO}_4^{2-}/\gamma\text{-Al}_2\text{O}_3$  for methanol dehydration reaction declined successively with increasing calcination temperature. The lower activity for methanol dehydration limited the conversion of methanol to DME, resulting in the lower DME selectivity and the lower CO conversion due to the reason given above. Especially, when the calcination temperature was increased to  $750\text{ }^{\circ}\text{C}$ , the DME selectivity and CO conversion declined markedly. As a result, the yield of DME was decreased to less than 40%.

The effect of the calcination temperature of  $\text{SO}_4^{2-}/\gamma\text{-Al}_2\text{O}_3$  on the performance of the hybrid catalysts containing sulfate-modified aluminas can also be attributed to the acidity changes of  $\text{SO}_4^{2-}/\gamma\text{-Al}_2\text{O}_3$  that occurred in the calcination process. Relatively stronger acid sites generated on  $\text{SO}_4^{2-}/\gamma\text{-Al}_2\text{O}_3$  catalyst calcined at  $\leq 450\text{ }^{\circ}\text{C}$ , as shown in Fig. 3, should be responsible for the formation of larger amount of  $\text{CO}_2$  due to the water reforming reactions of methanol and dimethyl ether as suggested by Joo et al. [10]. They found that when H-ZSM-5 with large number of strong acid sites was used as a dehydrating component,  $\text{CO}_2$  became the major product, which resulted in very poor DME selectivity (13.3%). The strength of acid sites of the  $\text{SO}_4^{2-}/\gamma\text{-Al}_2\text{O}_3$  was decreased as the calcination temperature increased, and thus the reforming reaction of methanol and DME to form  $\text{CO}_2$  was decreased [10]. As a consequence, both the DME selectivity and CO conversion increased. However, the further increase in calcination temperature ( $\geq 550\text{ }^{\circ}\text{C}$ ) greatly decreased both the strength and the numbers of acid sites

of the  $\text{SO}_4^{2-}/\gamma\text{-Al}_2\text{O}_3$  samples, so that the methanol produced by CO hydrogenation cannot be converted effectively to DME, resulting in lower DME selectivity and lower CO conversion due to the reason given above. This result further suggests that when the overall reaction is controlled by the methanol dehydration reaction, the higher the acidity of the dehydrating catalyst is, the higher the CO conversion and DME selectivity will be.

### 3.3. Catalyst stability

In order to investigate the stability of the hybrid catalysts with sulfate-modified alumina as methanol dehydration components in the STD process, the catalyst containing (10 wt.%)  $\text{SO}_4^{2-}/\gamma\text{-Al}_2\text{O}_3$  calcined at  $550\text{ }^{\circ}\text{C}$  was evaluated over an 80 h period, in which the reactor was operated continuously under the test conditions. The changes of the CO conversion and the DME selectivity in the organic products as a function of reaction time are depicted in Fig. 4. It clearly shows that both the DME selectivity and the CO conversion remained essentially constant for the whole test period, which indicates that no substantial deactivation of the catalyst occurred. This result reveals that the hybrid catalyst containing the  $\text{SO}_4^{2-}/\gamma\text{-Al}_2\text{O}_3$  with 10 wt.% sulfate and calcined at  $550\text{ }^{\circ}\text{C}$  has good stability for the direct synthesis of DME from syngas.

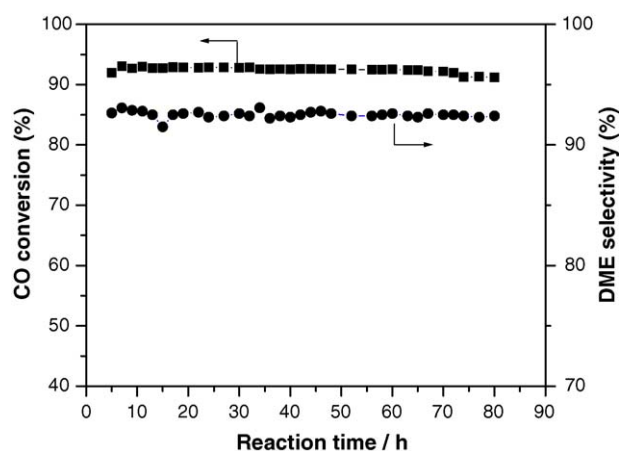


Fig. 4. Long-term test of activity and selectivity of the hybrid catalyst with  $\gamma\text{-Al}_2\text{O}_3$  modified with 10 wt.% sulfate and calcined at  $550\text{ }^{\circ}\text{C}$  as dehydration component. Reaction conditions:  $T = 260\text{ }^{\circ}\text{C}$ ,  $P = 4\text{ MPa}$ ,  $\text{H}_2/\text{CO} = 2.2$ ,  $\text{CO}_2 = 4\%$ ,  $\text{GHSV} = 1500\text{ ml h}^{-1}\text{ g}^{-1}$ .

#### 4. Conclusions

A series of catalysts,  $\text{SO}_4^{2-}/\gamma\text{-Al}_2\text{O}_3$ , were prepared by the impregnation method using an aqueous solution of ammonium sulfate and used as methanol dehydration components of the hybrid catalysts. It has been demonstrated that  $\text{SO}_4^{2-}/\gamma\text{-Al}_2\text{O}_3$  is a novel effective acid component for the hybrid catalyst applied in the direct synthesis of dimethyl ether from syn-gas. The hybrid catalyst containing the  $\text{SO}_4^{2-}/\gamma\text{-Al}_2\text{O}_3$  with 10 wt.% sulfate content and calcined at 550 °C exhibited the highest selectivity and yield for dimethyl ether synthesis. The enhanced catalytic activity of  $\gamma\text{-Al}_2\text{O}_3$  for methanol dehydration was related to the increase in the number and strength of acid sites owing to the addition of sulfate.

#### Acknowledgements

Financial support (Grant No. 200002) provided by China Petroleum and Chemical Corporation (SINOPEC) is gratefully acknowledged. The authors also wish to thank Shanghai Research Institute of Petrochemical Technology (SRIPT), SINOPEC, for the permission to publish this article. The helpful suggestions and the linguistic revision of the manuscript provided by the editor (Prof. Takashi Tatsumi) and the anonymous reviewers are also gratefully acknowledged.

#### References

- [1] W.W. Kaeding, S.A. Butter, *J. Catal.* 61 (1980) 155.
- [2] G. Cai, Z. Liu, R. Shi, C. He, L. Yang, C. Sun, Y. Chang, *Appl. Catal. A* 125 (1995) 29.
- [3] T. Shikada, K. Fujimoto, M. Miyauchi, H. Tominaga, *Appl. Catal. A* 7 (1983) 361.
- [4] N. Inoue, Y. Ohno, *Petrotech* 24 (2001) 319.
- [5] K. Fujimoto, K. Asami, T. Shikada, H. Tominaga, *Chem. Lett.* (1984) 2051.
- [6] J.B. Hansen, F. Joensen, *Stud. Surf. Sci. Catal.* 61 (1991) 457.
- [7] T. Takeguchi, K. Yanagisawa, T. Inui, M. Inoue, *Appl. Catal. A* 192 (2000) 201.
- [8] A.C. Sofianos, M.S. Scurrell, *Ind. Eng. Chem. Res.* 30 (1991) 2372.
- [9] K. Omata, Y. Watanabe, T. Umegaki, G. Ishiguro, M. Yamada, *Fuel* 81 (2002) 1605.
- [10] O.S. Joo, K.D. Jung, S.H. Han, *Bull. Korean Chem. Soc.* 23 (2002) 1103.
- [11] J.H. Kim, M.J. Park, S.J. Kim, O.S. Joo, K.D. Jung, *Appl. Catal. A* 264 (2004) 37.
- [12] K. Klier, *Adv. Catal.* 31 (1982) 243.
- [13] J. Nakamura, Y. Choi, T. Fujitani, *Topics Catal.* 22 (2003) 277.
- [14] X.M. Liu, G.Q. Lu, Z.F. Yan, J. Beltramini, *Ind. Eng. Chem. Res.* 42 (2003) 6518.
- [15] J.L. Li, X.G. Zhang, T. Inui, *Appl. Catal. A* 147 (1996) 23.
- [16] J.L. Li, X.G. Zhang, T. Inui, *Appl. Catal. A* 164 (1997) 303.
- [17] K.L. Ng, D. Chadwick, B.A. Toseland, *Chem. Eng. Sci.* 54 (1999) 3587.
- [18] J. Yagi, T. Akiyama, A. Muramatsu, *Stud. Surf. Sci. Catal.* 133 (2001) 435.
- [19] G. Qi, J. Fei, X. Zheng, Z. Hou, *React. Kinet. Catal. Lett.* 73 (2001) 245.
- [20] G. Qi, X. Zheng, J. Fei, Z. Hou, *J. Mol. Catal. A* 176 (2001) 195.
- [21] Q. Ge, Y. Huang, F. Qiu, S. Li, *Appl. Catal. A* 167 (1998) 23.
- [22] K. Sun, W. Lu, F. Qiu, S. Liu, X. Xu, *Appl. Catal. A* 252 (2003) 243.
- [23] J. Xia, D. Mao, B. Zhang, Q. Chen, Y. Tang, *Catal. Lett.* 98 (2004) 235.
- [24] H. Xiu, Q. Ge, W. Li, S. Hou, C. Yu, M. Jia, *Stud. Surf. Sci. Catal.* 136 (2001) 33.
- [25] J. Xia, D. Mao, N. Xu, Q. Chen, Y. Zhang, Y. Tang, *Chem. Lett.* 33 (2004) 1456.
- [26] M. Xu, J.H. Lunsford, D.W. Goodman, A. Bhattacharyya, *Appl. Catal. A* 149 (1997) 289.
- [27] L.D. Brake, US Patent, 4,595,785 (1986), to E.I. DuPont de Nemours and Company.
- [28] K.W. Jun, H.S. Lee, H.S. Roh, S.E. Park, *Bull. Korean Chem. Soc.* 23 (2002) 803.
- [29] F. Yaripour, F. Baghaei, I. Schmidt, J. Perregaard, *Catal. Commun.* 6 (2005) 147.
- [30] P. Berteau, B. Delmon, *Catal. Today* 5 (1989) 121.
- [31] T. Curtin, J.B. McMonagle, B.K. Hodnett, *Appl. Catal.* 93 (1992) 75.
- [32] K. Arata, M. Hino, *Appl. Catal.* 59 (1990) 197.
- [33] T. Yang, T. Chang, C. Yeh, *J. Mol. Catal. A* 115 (1997) 339.
- [34] H. Matsuhashi, D. Sato, K. Arata, *React. Kinet. Catal. Lett.* 81 (2004) 183.
- [35] M. Marczewski, A. Jakubiak, H. Marczevska, A. Frydrych, M. Gontarz, A. Sniegula, *Phys. Chem. Chem. Phys.* 6 (2004) 2513.
- [36] D.E. Gawthorpe, A.F. Lee, K. Wilson, *Phys. Chem. Chem. Phys.* 6 (2004) 3907.
- [37] D. Mao, Q. Song, B. Zhang, W. Yang, CN Patent, 1,657,163 (2004), to China Petroleum and Chemical Corporation (SINOPEC).
- [38] D. Mao, Q. Song, B. Zhang, W. Yang, CN Patent, 1,657,515 (2004), to China Petroleum and Chemical Corporation (SINOPEC).
- [39] D. Mao, W. Yang, J. Xia, B. Zhang, Q. Song, Q. Chen, *J. Catal.* 230 (2005) 140.
- [40] J.R. Sohn, W.C. Park, *Appl. Catal. A* 239 (2003) 269.
- [41] A.N. Ko, C.L. Yang, W.D. Zhu, H.E. Lin, *Appl. Catal. A* 134 (1996) 53.
- [42] J.C. Chang, A.N. Ko, *React. Kinet. Catal. Lett.* 83 (2004) 283.
- [43] N. Li, A. Wang, L. Li, X. Wang, L. Ren, T. Zhang, *Appl. Catal. B* 50 (2004) 1.
- [44] J.J. Spivey, *Chem. Eng. Comm.* 110 (1991) 123.
- [45] F. Abbattista, S. Delmastro, G. Gozzelino, D. Mazza, M. Vallino, G. Busca, V. Lorenzelli, G. Ramis, *J. Catal.* 117 (1989) 42.
- [46] C.D. Chang, A.J. Silvestri, *J. Catal.* 47 (1977) 249.
- [47] N.S. Figoli, S.A. Hillar, J.M. Parera, *J. Catal.* 20 (1971) 230.
- [48] F.S. Ramos, A.M. Duarte de Farias, L.E.P. Borges, J.L. Monteiro, M.A. Fraga, E.F. Sousa-Aguiar, L.G. Appel, *Catal. Today* 101 (2005) 39.